# Experiments on a Turbulent Jet in a Cross Flow

YASUHIRO KAMOTANI* AND ISAAC GREBER†
*Case Western Reserve University, Cleveland, Ohio*

**Results are reported of experiments on turbulent circular jets issuing into a cross flow, both for unheated and heated jets. Longitudinal and transverse distributions of velocity, temperature, and turbulence intensity are presented. The velocity distributions depend mainly on the ratio of jet to cross flow momentum flux. The temperature distributions depend also on the density ratio. The jet structure is dominated by a vortex wake which forms behind the jet, which is evident both from the detail measurements and from smoke photographs of the flow. The experiments also indicate that the components of cross flow normal and parallel to the jet trajectory independently control the entrainment rate.**

## Introduction

THE work reported herein was motivated by the need to cool combustion gases in gas turbine combustors. Generally, cooling is done by injecting relatively cool air through holes in the surrounding wall. Although more than one jet is used for effective cooling, a single jet is investigated first to give basic information for the combustor cooling and other applications. The experiments with the jet and freestream at different temperatures are made with the jet hotter than the freestream, because it is experimentally simpler. The results of the unheated and heated jet experiments are expected to be applied deductively to the cooling problem. The results also have application to other problems such as the structure of plumes from chimneys, V/STOL aircraft using air jets to obtain lift for takeoff, etc.

Because of their importance in a variety of applications, unheated jet experiments have been conducted by a number of investigators. Among these, Jordinson[1] measured total pressure distributions at several jet cross sections, Keffer and Baines[2] investigated some features of the velocity field in the jet upstream region, and Margason[3] made measurements of the jet trajectory and summarized the available information on trajectories.

Much less information is available on heated jet behavior. Pertinent to the present work are the early attempts by Callaghan and Ruggeri[4,5] to correlate temperature distributions in the plane of symmetry of the jet, and the experiments of Ramsey and Goldstein[6] which investigate velocity and temperature distributions in cross-sectional planes as well as in the plane of symmetry, for very small momentum ratios.

The present work on unheated jets can be regarded as extending the Keffer and Baines work to farther downstream regions, and includes a detailed investigation of the circulating flow in the cross-planes. This circulating flow forms a vortexlike structure, which is the dominant feature of the downstream jet. From the detailed velocity measurements an analysis is made of the entrainment rate and its importance in determining the jet structure. The present work on heated jets is for momentum ratios considerably higher than those reported by Ramsey and Goldstein, and cover a larger downstream region. To supplement the measurements, smoke photographs were taken, which visually show the jet shape distortion and the vortex structure.

Presented as Paper 72-149 at the AIAA 10th Aeros pace Sciences Meeting, San Diego, Calif., January 17-19, 1972; submitted January 26, 1972; revision received May 24, 1972. This work was supported by NASA through Grant NGR-36-027-008. The authors wish to acknowledge the inception of this work by the late H. K. Wiskind.

Index category: Jets, Wakes, and Viscous-Inviscid Flow Interactions

* Research Associate, Fluid, Thermal and Aerospace Sciences Division.

† Professor of Engineering, Fluid, Thermal and Aerospace Sciences Division, Member AIAA.

## Experimental Technique

Most of the experiments were performed in a 28 in. square cross section subsonic wind tunnel. Test section air velocities ranged from about 20 to 30 fps, and the freestream turbulence intensity was about 0.3%. The jet was injected perpendicularly to the freestream from a nozzle with a $\frac{1}{4}$ in. exit diameter. Special care was taken to obtain flat velocity profiles and low turbulence intensity (0.3%) at the jet nozzle exit. In order to minimize the effect of tunnel wall boundary layer the jet nozzle exit was placed flush with a flat plate placed 2.5 in. above the bottom wall of the tunnel. The plate was 17 in. wide and 24 in. long, with a sharp leading edge, and the jet nozzle was placed 2 in. downstream from the leading edge. For the hot jet experiments, air was heated using an electrical heating tape wrapped around a portion of the jet supply pipe, and thermally insulating the remainder of the supply pipe. The temperature profiles at the jet nozzle exit were very flat. A diagram of a portion of the test section with the flat plate in place is shown in Fig. 1. Smoke visualization experiments were performed both in the wind tunnel used for the quantitative experiments and also in two smaller tunnels.

Velocity and turbulence intensity were measured by a hot wire probe operated by a Shapiro and Edwards Model 50 constant-current hot wire anemometer. The mean flow direction was measured by a small yaw angle meter made of two hypodermic needles of 0.028 in. diam with beveled open ends. To measure three dimensional flow direction this yaw meter requires measurements in two planes at a given point. Temperature was measured using an iron-constantan thermocouple.

Detailed measurements were performed using jets having momentum fluxes ranging from about 15 to 60 times the cross-flow momentum flux. Jet trajectories were measured for momen-

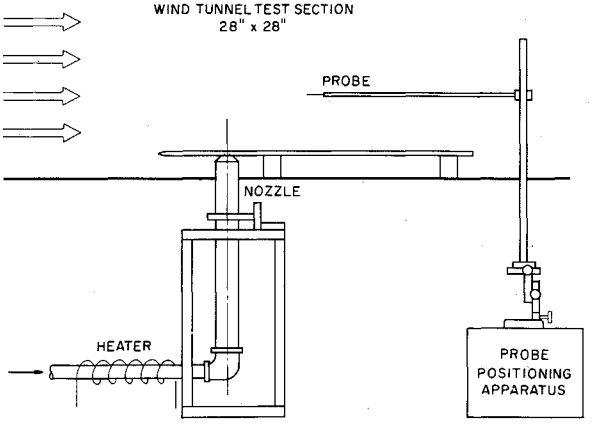


**Fig. 1 Sketch of test apparatus**

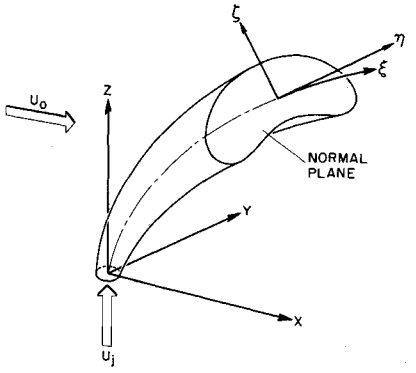


**Fig. 2 Sketch of jet in cross flow.**

tum ratios up to 570. The heated jet experiments were performed using initial jet temperatures up to about 400°F, and room temperature cross flow.

## Results of Measurements

*Velocity and Temperature Trajectories*

The jet velocity trajectory used herein is the locus of the maximum velocity in the plane of symmetry. This is the most common measure of jet trajectory used in experiments. For analytical purposes a mass-flux center path might be more useful, but this is quite difficult to obtain cleanly from experiments. A sketch defining the coordinate system based on the jet velocity trajectory is shown in Fig. 2. The jet temperature trajectory used herein is the locus of the maximum temperature in the plane of symmetry.

In these experiments the jet motion is inertially dominated, with buoyancy playing only a minor role. The result is that the trajectory depends mainly upon the ratio of the jet momentum flux to the freestream momentum flux (herein called the momentum ratio, $J = \rho_j U_j^2/\rho_0 U_0^2$) both for heated and for unheated jets. The temperature trajectory also appears to have a weak dependence on density ratio itself. Typical correlations of jet velocity and temperature trajectories with momentum ratio displaying the above features are shown in Fig. 3, for two momentum ratios and for two density ratios. It is seen that the temperature trajectories fall below the velocity trajectories.

In Fig. 3 and elsewhere the subscript "$v$" denotes velocity, the subscript "$T$" denotes temperature, and $D$ is the jet nozzle diameter. Note here and in the remainder of this work the Reynolds number range is from about 2800 to 4200, based on freestream conditions and jet nozzle diameter. In this range the effect of Reynolds number is not found to be important.

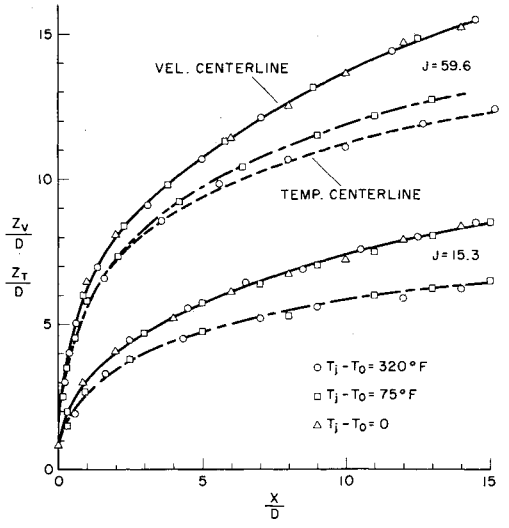


**Fig. 3 Velocity and temperature centerline location.**

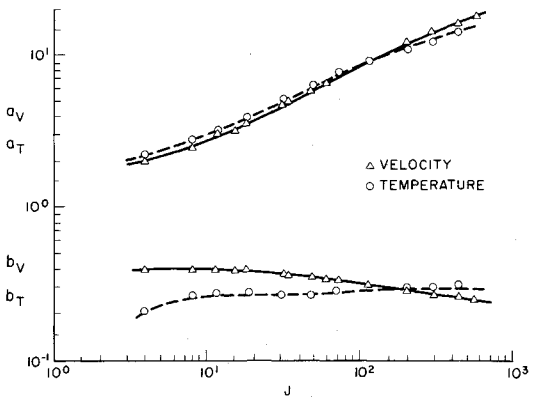


**Fig. 4 $a_V$, $b_V$, $a_T$ and $b_T$ vs $J$.**

In order to assess the importance of initial conditions on the trajectory, sample measurements were made using the nozzle without the flate plate, and using ordinary pipes of two different diameters instead of the nozzle, for one momentum ratio. The velocity trajectories show a spread of about 12% based on the mean values.

The correlations of the velocity and temperature trajectories can be expressed by the simple formulas

$$z_v/D = a_v(x/D)^{b_v}; \qquad z_T/D = a_T(x/D)^{b_T} \tag{1}$$

where $a_v$, $b_v$, $b_T$ are functions of the momentum ratio and $a_T$ depends mainly on the momentum ratio and weakly upon the density ratio itself. Figure 4 shows the values of $a_v$ and $b_v$ for the momentum ratio range 4–570, and the values of $a_T$ and $b_T$ for the momentum ratio range 4 to 450 and the fixed density ratio $\rho_j/\rho_0 = 0.73$, for $x/D$ between zero and 20.

In restricted ranges of the momentum ratio, the velocity and temperature trajectories written in the form of Eq. (1) can each be reduced to a single curve by choosing approximate constant values of $b_v$, $b_T$ and approximate functional forms of $a_v$, $a_T$. Such a reduction is possible for the entire range of momentum ratios, $J$ from about 15 to 60, for which detailed measurements were made in this work. The correlation is shown in Fig. 5. Also shown on Fig. 5 is the spread of velocity trajectory data obtained from Margason's[3] summary and presented in accordance with the present correlation. The spread is large because of the large variation in the kinds of experiments and the definitions of the trajectory. It includes trajectories obtained from smoke pictures, pitot tube measurements, and jets issuing from tubes protruding far into the cross flow. The data taken by Keffer and Baines[2] are based on the same definition and physical situation as the present work; their data very closely follows the present results, but was only obtained for $x/D < 4$.

Very near the nozzle exit the jet exhibits a so-called "potential core" in which the velocity is nearly uniform. In this region the definition of the jet trajectory as the locus of maximum velocity

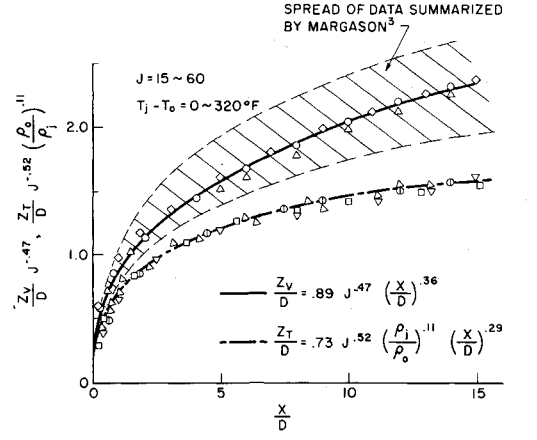


**Fig. 5 Correlation of velocity and temperature centerline profiles.**

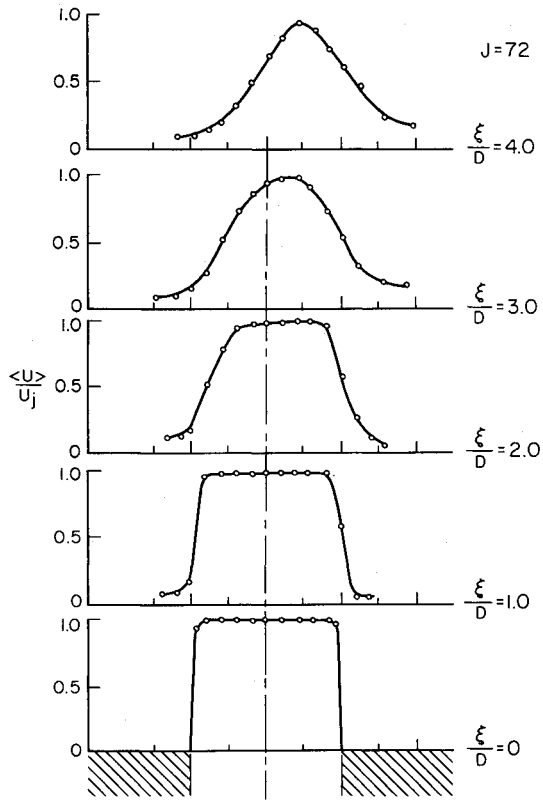


Fig. 6 Velocity distribution in jet initial region.

is not directly useful. Without examining the local behavior near the nozzle, one tends to "observe" that the jet deflection starts not at the nozzle exit but at some point above it, usually called the "effective source of jet deflection." However, measurements of velocity profiles near the jet exit, shown in Fig. 6, show that the jet deflects very close to the nozzle, and suggests that the "effective source" idea is misleading and the expression of Eq. (1) is more realistic.

*Velocity Distribution in Cross Planes*

As the jet enters a cross flow its shape begins to change because of the nonuniform pressure field created by the flow around it. The jet is deformed into a crescent shape, and the cross flow creates a pair of vortices behind the jet in much the same way as a flow around a cylinder. The vortices acquire axial momentum from the jet, and move along the jet path while increasing their strength. Far downstream the original jet disappears, while a pair of vortices dominate the flowfield.

Measurement of velocity is not simple because of the three-dimensional flow. However, because the flow directions are nearly parallel in the $x$-$y$ plane, a hot wire aligned with $y$ axis measures a speed close to the correct one. The time average speed $\langle U \rangle$ so measured is here nondimensionalized as

$$\tilde{u} = (\langle U \rangle - U_0)/(\langle U \rangle_{\max} - U_0) \qquad (2)$$

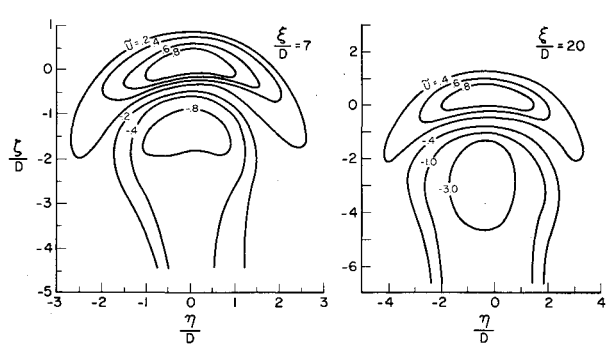


Fig. 7 Contours of constant velocity ($J$ = 15.3).

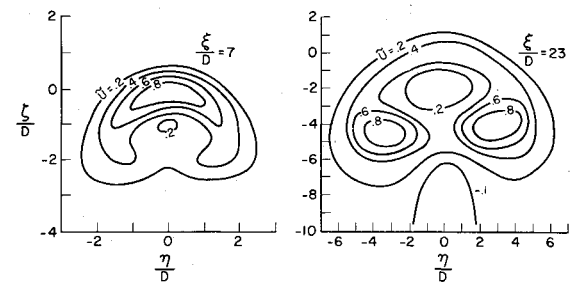


Fig. 8 Contours of constant velocity ($J$ = 59.6).

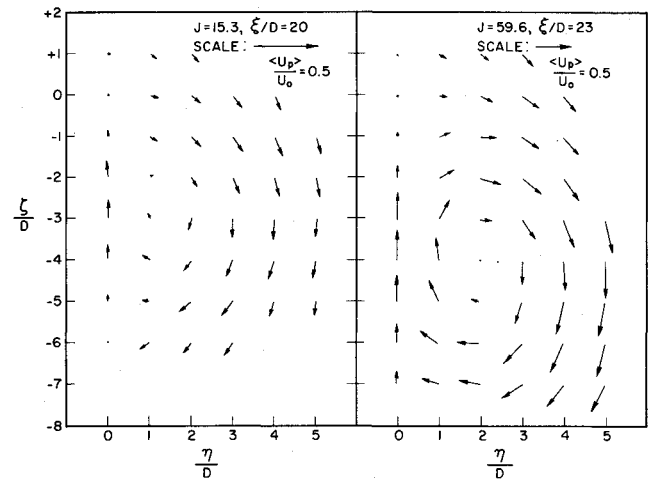


Fig. 9 Projection of velocity vectors on normal plane.

where $\langle U \rangle_{\max}$ is the maximum speed in a given normal plane and $U_0$ is the cross flow speed. Figures 7 and 8 show contours of constant $\tilde{u}$ (or $\langle U \rangle$) at an upstream and a downstream location for two momentum ratios. At the lower momentum ratio, $J = 15.3$, the jet is bent so sharply that vortices do not have time to develop, and the vortices are everywhere weak. Consequently the crescent-shaped jet is preserved into the far downstream region. At the higher momentum ratio, $J = 59.6$, the vortices are stronger, and the vortex structure becomes the dominant feature of the downstream region, as is apparent in the figure. Figure 9 shows the projection of the velocity vectors on the normal plane $U_p$ which closely represents the circulating velocity field. Again the vortical structure is very clear. Comparison of data at other locations shows that the vortex strength increases with $\xi$ up to some point, then decays because of viscous action. One sees from figures like 8 and 9 that although the

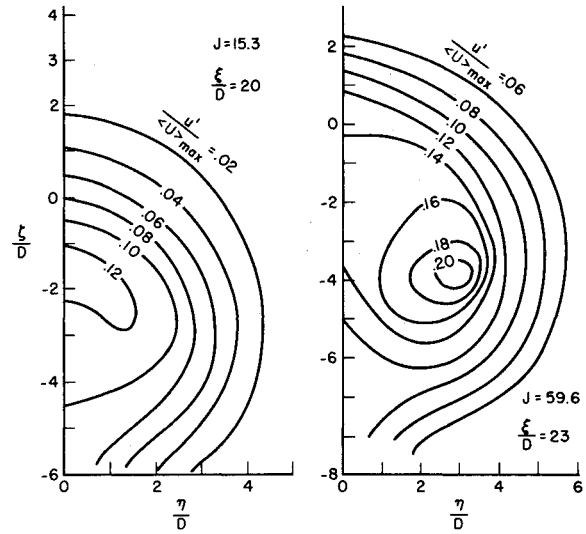


Fig. 10 Distribution of turbulence intensity.

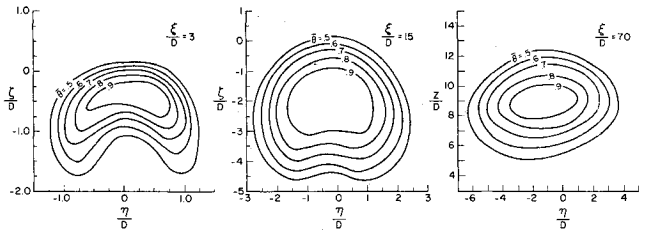

Fig. 11 Contours of constant temperature; $J = 15.3$, $T_j - T_0 = 320°F$.

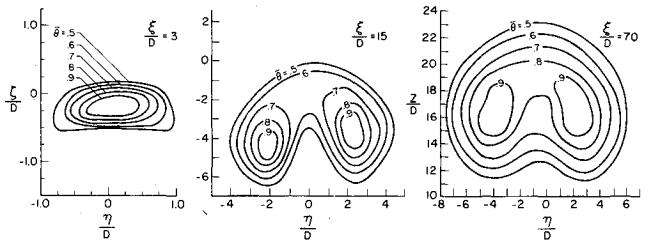

Fig. 12 Contours of constant temperature; $J = 59.6$, $T_j - T_0 = 320°F$.

magnitudes of the circulating secondary velocities are small they are associated with dramatic shifting of the maximum velocity location, from the midplane to the vortex centers.

The lateral distribution of turbulence intensity for an unheated jet is shown in Fig. 10. The turbulence level as a whole increases with increasing momentum ratio. This turbulence field and the circulating velocity field mainly determine the distributions of momentum and temperature.

## Temperature Distributions in Cross Planes

The temperature is made dimensionless in a manner similar to the velocity:

$$\bar{\theta} = (\langle T \rangle - T_0)/(\langle T \rangle_{\max} - T_0) \tag{3}$$

Figures 11 and 12 show contours of constant $\bar{\theta}$ (or $\langle T \rangle$) for two momentum ratios and three axial locations. Note that the temperature distribution can be measured much farther downstream than the velocity distribution.

The temperature spreads quickly into the vortex region, and for the lower momentum ratio, $J = 15.3$, the temperature distribution becomes nearly axisymmetric, which is quite different from the velocity distribution. For the higher momentum ratio, $J = 59.6$, the vortex action is stronger and the vortical structure is mirrored in the temperature distribution. As with the velocity, the vortical motion is associated with temperature maxima near the vortex centers rather than on the plane of symmetry. Temperature distributions in cross planes, at the same momentum ratio but at different density ratios, indicate that there is a separate effect of density ratio, as appeared in the examination of temperature trajectories. This may be due to a slight increase of entrainment rate with decreasing density ratio, as suggested by Ricou and Spalding.[7]

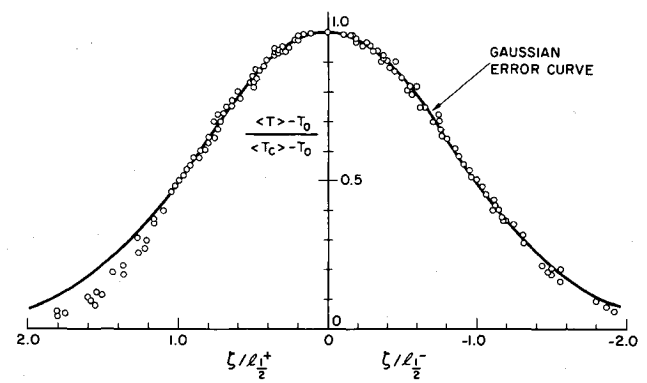


Fig. 13 Temperature distribution in the plane of symmetry.

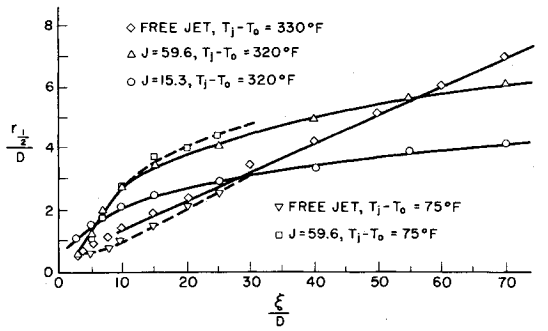


Fig. 14 Lateral spread of temperature in jet.

Figure 13 shows the transverse distribution of temperature in the plane of symmetry, for a large number of experiments at different conditions. They show a remarkable self-similarity, when the transverse distance is stretched with a local characteristic length, here taken as the distance from maximum temperature, in the plane of symmetry, to half the maximum.

## Jet Spread and Decay

As a measure of lateral spread of temperature, the half-value radius $r_{1/2}$ is introduced, defined as

$$r_{1/2} = (S_{1/2}/\pi)^{1/2} \tag{4}$$

where $S_{1/2}$ is the area occupied by the contour of $\bar{\theta} = 0.5$. Figure 14 shows the axial distribution of $r_{1/2}$ for $J = 15.3$ and 59.6. Also shown is the spreading rate of temperature in a freejet for comparison. One sees that initially the temperature in a jet in a cross flow spreads faster than in a freejet, but farther downstream approaches the freejet spread rate. The corresponding decay of maximum temperature with $\xi$ is shown in Fig. 15. As seen in the figure, the decay is faster than in a freejet, which also corresponds to the more rapid spreading of the jet in a cross flow. Upstream the decay is faster for smaller momentum ratios, but downstream the decay is nearly independent of momentum ratio.

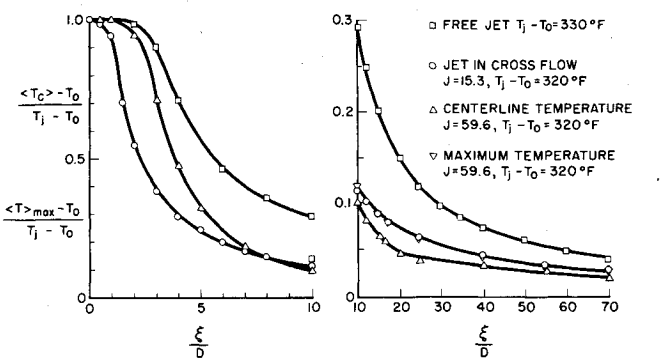


Fig. 15 Decay of temperature with distance from nozzle.

Fig. 16 Photographs of jets in cross flow.

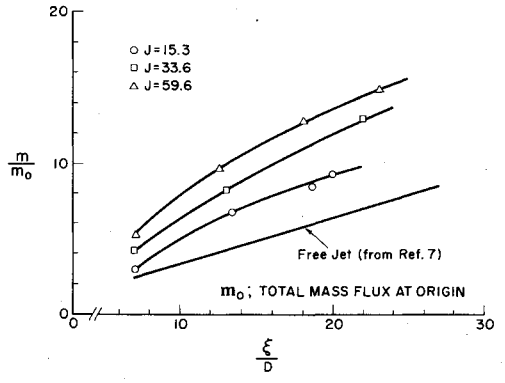


**Fig. 17 Mass flux distribution; a) turbulent jet, b) laminar jet.**

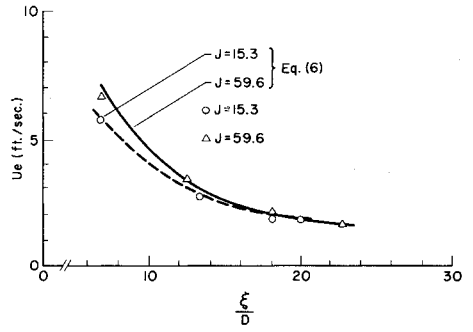


**Fig. 18 Entrainment velocity distribution.**

## Smoke Visualization

Photographs were taken, injecting kerosene smoke into the jet and illuminating a narrow layer of jet cross section. Two typical photographs are shown in Fig. 16, one for turbulent flow corresponding to the measurements, and one for laminar flow. The turbulent flow photograph suggests the structure elucidated by the measurements; the laminar flow photograph shows the vortices very clearly.

Additional data and photographs are shown in Ref. 8, from which most of the data presented herein are taken.

## Entrainment Analysis

In a turbulent jet or wake, mass flux within the turbulent region increases by entraining outside fluid as the fluid mass moves downstream. The rate of increase of the total mass flux in the turbulent region is given by

$$dm/d\xi = \rho_0 l U_e \tag{5}$$

where $\rho_0$ is the density of the outside fluid, $l$ is the perimeter of the turbulent region at $\xi$, and $U_e$ is the velocity (averaged over the circumference) at which the turbulent front is advancing into the outer region at $\xi$. From the measured velocity distributions, the mass flux was calculated for the region where the normal velocity excess is more than 10% of the maximum value at a given station. The result is shown in Fig. 17 for three momentum ratios.

In usual turbulent flow analyses, $U_e$ is assumed to be proportional to the local characteristic velocity scale, and the proportionality constant is called the entrainment coefficient. For a jet in a cross flow the choice of the characteristic velocity is not simple, because the two fluids are not parallel. Becuase the component of the cross flow velocity parallel to the cross-plane, $U_{op}$, controls the rotational velocity field, it is reasonable to introduce two entrainment coefficients such that

$$\begin{aligned} U_e &= E_1(\langle U\rangle_{\max} - U_{on}) + E_2 U_{op} \\ &= E_1(\langle U\rangle_{\max} - U_0\cos\theta) + E_2 U_0 \sin\theta \end{aligned} \tag{6}$$

where $\theta$ is the angle of inclination of the jet velocity trajectory. Since the flow structure changes as one changes the momentum ratio, values of both $E_1$ and $E_2$ are expected to be different for different momentum ratios. However, for a given momentum ratio both $E_1$ and $E_2$ are supposed to be constant in the region where the structural similarity is nearly preserved, which in these experiments is true for $J = 15.3$ and 59.6.

Figure 18 shows distributions of $U_e$ calculated from the measured values of $m$, $l$, $\rho_0$ and also as determined from Eq. (6) with $E_1 = 0.070$ and $E_2 = 0.320$ for $J = 15.3$, and $E_1 = 0.067$ and $E_2 = 0.182$ for $J = 59.6$. The ability to find a single pair $E_1$, $E_2$ for a single momentum ratio does not prove the validity of Eq. (6), but at least suggests that the normal and parallel flows independently control the entrainment rate.

The same kind of analysis, treating normal and tangential flowfields independently, can be applied to the flowfield very near the nozzle. The predicted potential core length agrees well with the measured value.[8]

## Conclusions

1) The jet velocity and temperature trajectories are mainly determined by the momentum ratio. The temperature trajectory is also weakly dependent upon the density ratio. 2) A pair of vortices forms behind the jet soon after it emerges from the nozzle, and strongly interacts with the jet. The downstream temperature and velocity distributions are in major part determined by the vortex motion. 3) The entrainment process is nearly independently controlled by the normal and parallel components of the velocity. 4) Turbulence intensity increases with increasing momentum ratio. The turbulence intensity distribution is qualitatively similar to the temperature distribution.

## References

[1] Jordinson, R., "Flow in a Jet Directed Normal to the Wind," R and M 3074, Oct. 1956, Aeronautical Research Council, Great Britain.

[2] Keffer, J. F. and Baines, W. D., "The Round Turbulent Jet in a Cross-Wind," *Journal of Fluid Mechanics*, Vol. 15, Pt. 4, 1963, pp. 481–496.

[3] Margason, R. J., "The Path of a Jet Directed at Large Angles to a Subsonic Free Stream," TN D–4919, 1968, NASA.

[4] Callaghan, E. E. and Ruggeri, R. S., "Investigation of the Penetration of an Air Jet Directed Perpendicularly to an Air Stream," TN–1615, 1948, NACA.

[5] Callaghan, E. E. and Ruggeri, R. S., "A General Correlation of Temperature Profiles Downstream of a Heated Jet Directed Perpendicularly to an Air Stream," TN–2466, 1951, NACA.

[6] Ramsey, J. W. and Goldstein, R. J., "Interaction of a Heated Jet with a Deflecting Stream," Rept. 71–HT–2, 1971, ASME.

[7] Ricou, F. P. and Spalding, D. B., "Measurements of Entrainment by Axisymmetrical Turbulent Jets," *Journal of Fluid Mechanics*, Vol. 11, Pt. 1, 1961, pp. 21–32.

[8] Kamotani, Y. and Greber, I., "Experiments on a Turbulent Jet in a Cross Flow," Rept. FTAS/TR–71–62, 1971, Div. of Fluid, Thermal, and Aerospace Sciences, Case Western Reserve Univ., Cleveland, Ohio; also CR–72893, 1971, NASA.